Fam, Amin Moghimy; Lehtonen, Matti; Pourakbari-Kasmaei, Mahdi; Fotuhi-Firuzabad, Mahmud

Optimal Sizing of a Wind-PV Grid-Connected Hybrid System for Base Load- Helsinki Case

Published in:
2023 19th International Conference on the European Energy Market, EEM 2023

DOI:
10.1109/EEM58374.2023.10161955

Published: 01/01/2023

Document Version
Peer-reviewed accepted author manuscript, also known as Final accepted manuscript or Post-print

Optimal Sizing of a Wind-PV Grid-Connected Hybrid System for Base Load– Helsinki Case

Amin Moghimy Fam, Matti Lehtonen, Mahdi Pourakbari-Kasmaei
Dept. Electrical Engineering and Automation
Aalto University
Espoo, Finland
amin.moghimyfam@aalto.fi, matti.lehtonen@aalto.fi, Mahdi.Pourakbari@aalto.fi

Mahmud Fotuhi-Firuzabad
Dept. Electrical Engineering
Sharif University of Technology
Tehran, Iran
fotuhi@sharif.edu

***Abstract*-- In recent years, due to the goal of decarbonizing energy systems, Renewable Energy Sources (RESs) have attracted attention as the primary potential energy resource in many countries. Thus, the utility-scale deployment of these resources has become of utmost importance. The large-scale connections and the intermittent as well as variable characteristics of these RESs cause challenges in maintaining a balance between power generation and consumption. Furthermore, supplying base load using RESs is another challenge for system operators. Hybrid RESs (HRESs), including solar and wind, together with energy storage, might be a remedy via which the resources can complement each other to some extent. In this paper, using geographical data acquired from National Solar Radiation Database and Matlab/Simulink, the output of each individual solar panel and wind turbine unit in the Helsinki region are calculated and used to optimally size an HRES to supply the base load. The results indicate that an HRES is at least 10.5 times more cost-efficient compared to a single RES system. Furthermore, it can be seen that, even in Finland where there is not sufficient solar radiation in winter, the size of the required energy storage system reduces by at least 13.4 times when an HRES is used.**

***Index Terms*— Hybrid energy system, PV, Renewable energy sources, Wind turbine.**

I. INTRODUCTION

Renewable energy sources (RESs), such as solar and wind, offer a clean and economically competitive alternative to conventional power generation, in which most of the energy is produced using fossil fuels with huge amounts of CO_2 emission. Producing energy with almost no CO_2 emission using RESs aligns with the EU goal of becoming net-zero greenhouse gas emission [1]. Although RES proposes a solution toward carbon neutrality, intermittent power output and other associated uncertainties raise many challenges for system planners and operators. In this regard, hybrid renewable energy systems (HRESs) are considered to be useful as they introduce a potential solution to overcome the challenges.

Solar and wind power are among the most popular RESs. These two sources can act in a complementary manner to smooth their intermittent power output. Hence, using a Wind-PV HRES introduces a beneficial approach to enhancing the economic and environmental sustainability of RESs and is usually more cost-efficient and reliable than a system with a single renewable energy source [2], [3].

In [4], to overcome the intermittent power output for producing hydrogen, the application of Wind-PV HRES, including a battery energy storage system (BESS), was introduced. The results show encouraging HRES efficiency compared to similar experimental systems. In [5], an HRES performance assessment procedure was proposed based on the IEC-61724. The authors in [6] presented a detailed standalone Wind-PV HRES sizing method and introduced a flexible software based on the Loss of Power Supply Probability (LPSP) algorithm and techno-economic analysis using object-oriented programming. In [7], a review of hybrid energy systems (HESs), consisting of both RES and conventional fossil fuel-based generators, was presented. Also, a case study was conducted to determine the most economical- and emission-optimal configuration of a PV, wind, BESS, and diesel generator HES in a remote area. In [8], a sizing method for Wind-PV HRES was proposed aiming at maximizing the annual ratio of the demand supplied by HRES to total demand with Levelized Cost of Energy (LCOE) being equal to the grid tariff, to meet both economic and environmental goals.

The authors in [9] proposed an optimal techno-commercial integration of PV, wind, Biomass, and Vanadium Redox flow battery (VRFB) in a Microgrid to satisfy the daily energy demand. The simulations were performed using Hybrid Optimization of Multiple Energy Resources (HOMER) and the PSCAD was used to validate the results. In [10], a study on a 6kW residential Wind-PV HRES was conducted where the results show that the system is economical and provides an opportunity for households to profit by implementing the HRES. In [11], the optimal sizing of a grid-connected Wind-PV-hydro HRES was investigated, aiming at minimizing the difference between HRES daily power output and load and maximizing HRES daily power generation. In [12], a genetic algorithm-based heuristic approach was developed for the

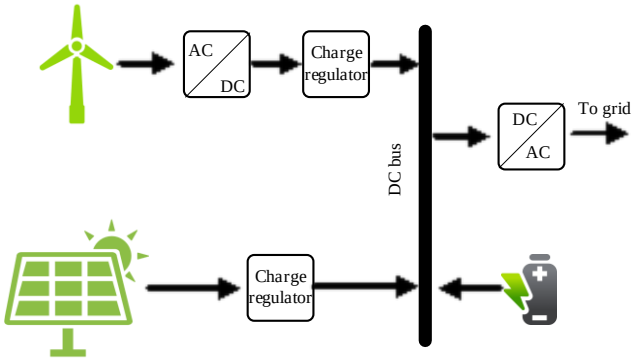

Figure 1: WT-PV hybrid system

optimal sizing of an HRES consisting of PV, wind, and BESS to minimize LCOE and LPSP. The work in [13] deployed a whale optimization algorithm (WOA) to optimally size an HRES consisting of PV, wind turbine (WT), tidal, fuel cell (FC), and hydrogen storage with minimum net present cost and cost of energy that satisfies reliability goals.

All these references introduced different approaches to optimally size an HRES, primarily to lower the investment costs to supply a load or lower the LCOE. However, none of them takes the base load into account. Conventionally, the base load is supplied by fossil fuel-based or nuclear power plants. On the other hand, considering the radical transition toward becoming net-zero carbon emission, the importance of supplying base load using RESs arises. RESs, due to their intermittent power output and being less predictable, impose a huge uncertainty on the system. Hence, this paper aims toward the optimal sizing of an HRES consisting of PV, WT, and BESS as the energy storage system. In this study, different scenarios for base load type are analyzed with a simplified formulation to identify the benefit of using HRES over a single-source renewable energy system, the associated costs and each component's contribution, and the required technology development toward becoming fully green electrified.

The rest of the paper is organized as follows. Section II provides the mathematical model of each component of the studied HRES. Section III represents the simplified formulation of the problem. Section IV presents the input data for the simulation. The simulation results and discussions are provided in Section V. Finally, Section IV concludes the paper.

II. Mathematical Model of HRES Components

In this section, the mathematical model of the grid-connected wind-PV HRES is demonstrated. The HRES in the proposed model consists of PV panels, WTs, and BESS, as depicted in Figure 1. Different components of the model are explained in detail in the following subsections.

A. PV Panel

The behavior of a PV panel can be modeled as a nonlinear current source with intrinsic cell series resistance. A PV module consists of several solar cells, which are basically a p-n diode. The output current of a PV cell mostly depends on solar radiation (G_T) and cell temperature (T_c). Hence, the illustrated model should provide an output of a PV cell considering both these factors. Considering the PV panel equipped with a maximum power point tracker (MPPT), the output power of a PV panel can be calculated using [14]–[16]:

$$I_{mpp} = I_{sc}.\left\{1 - C_1.\left[\exp\left(\frac{V_{mpp,r}}{C_2.V_{OC}}\right) - 1\right]\right\} + \Delta I \quad (1)$$

$$V_{mpp} = V_{mpp,r} + \alpha_{V_{OC}}.\Delta T \quad (2)$$

$$P_{mpp} = V_{mpp}.I_{mpp} \quad (3)$$

where,

$$C_1 = \left(1 - \frac{I_{mpp,r}}{I_{SC}}\right).\exp\left(-\frac{V_{mpp,r}}{C_2.V_{OC}}\right) \quad (4)$$

$$C_2 = \left(\frac{V_{mpp,r}}{V_{OC}} - 1\right).\left[\ln\left(1 - \frac{I_{mpp,r}}{I_{SC}}\right)\right]^{-1} \quad (5)$$

$$\Delta I = I_{SC}.\left(\frac{G_T}{G_{ref}} - 1\right) + \alpha_{I_{sc}}.\Delta T \quad (6)$$

$$\Delta T = T_c - T_{c,ref} \quad (7)$$

$$T_c = T_a + \frac{NOCT - 20}{800}.G_T \quad (8)$$

where I_{mpp}, V_{mpp}, and P_{mpp} are respectively the current, voltage, and output power of the PV panel at the maximum power point; I_{sc}, V_{OC}, $I_{mpp,r}$, and $V_{mpp,r}$ are respectively the short circuit current, open circuit voltage, maximum point current, and maximum point voltage at the reference point; $\alpha_{I_{sc}}$ is the short circuit current temperature coefficient; $\alpha_{V_{OC}}$ is the open circuit voltage temperature coefficient; G_T is the solar radiation; G_{ref} is the solar radiation at the reference point; T_c and $T_{c,ref}$ are the PV cell temperature and the PV cell temperature at the reference point, respectively; T_a is the ambient temperature, and $NOCT$ is the normal operating cell temperature when PV panel operates under 800 W/m^2 of solar radiation and at 20°C of ambient temperature. The utilized parameters in the model and reference points are usually provided in each PV panel datasheet. It should be noted that, in this study, converters' behavior has not been considered and only the maximum possible output of a PV panel is calculated.

Using the proposed mathematical model for a PV panel, the output power of a panel can be estimated at given solar radiation and ambient temperature at a given time as (9).

$$P_{PV}(t) = P_{mpp}(t) = I_{mpp}(t).V_{mpp}(t) \quad (9)$$

B. Wind Turbine

WT is another component of HRES. Characteristic curves for WTs are given as power output versus the wind speed at the hub height. The output power of a WT can be calculated using the swept blade area (A), the air density (ρ_a), the wind velocity (v), and the coefficient of power (C_p). The coefficient of power can be formulated depending on the design factors ($c_1 - c_6$) as follows.

$$C_p(\lambda, \vartheta) = c_1\left(c_2\frac{1}{\beta} - c_3\vartheta - c_4\vartheta^x - c_6\right)e^{-c_5/\beta} \quad (10)$$

where:

$$\lambda = r\omega m/v \quad (11)$$

$$\frac{1}{\beta}=\frac{1}{\lambda+0.08\vartheta}-\frac{0.035}{1+3\vartheta} \tag{12}$$

The power output of a WT can be expressed as (13).

$$P_w(t)=\frac{1}{2}C_p(\lambda,\vartheta)\rho_a A v^3(t) \tag{13}$$

However, this output power is achieved only for a certain range of wind speed. Generally, the WT output power is given by a datasheet that can be separated into four areas as follows.

1) The area where the wind speed is less than the cut-in wind speed (v_{ci}) of the WT. In this case, the WT generation is zero.
2) The area where wind speed is higher than the WT's cut-in speed (v_{ci}) and less than its nominal wind speed (v_n). In this case, WT generation is calculated using (13).
3) The area where wind speed is more than the WT's nominal wind speed (v_n) and less than its cut-out wind speed (v_{co}). In this case, WT generates its nominal output power (P_w^r).
4) The area where wind speed is higher than the WT's cut-out wind speed (v_{co}). In this case, WT does not generate any power.

These conditions can be summarized as (14).

$$P_w^{av}(t)=\begin{cases}0 & if\ v<v_{ci}\\ P_w(t)=\frac{1}{2}C_p(\lambda,\vartheta)\rho_a A v^3(t) & if\ v_{ci}\le v\le v_n\\ P_w^r & if\ v_n\le v\le v_{co}\\ 0 & if\ v>v_{co}\end{cases} \tag{14}$$

C. Battery Energy Storage System

Due to intermittent and not fully controllable generation of power sources in an HRES, an electrical energy storage system (EESS) seems to be imperative to maintain its optimal function. Hence, an EESS is needed for the proposed HRES to be able to inject adequate power into the grid to meet the base load. Therefore, in this paper, it is referred to as a BESS.

The main characteristic of a BESS is its state of charge (SOC), which reflects the level of stored energy in a BESS relative to its capacity at each time. Also, at a given time, the total generation of the HRES can be calculated as (15).

$$P_g(t)=P_w(t)+P_{PV}(t) \tag{15}$$

The SOC at each time ($SOC(t)$) for a 1-hour time step depends on the SOC at a time interval before ($SOC(t)$), the charging power ($P_{ch}(t)$), and discharging power ($P_{dis}(t)$). Hence, the SOC can be expressed as:

$$SOC(t)=SOC(t-1)*(1-\sigma)+\left[\eta_{ch}P_{ch}(t)-\frac{P_{dis}(t)}{\eta_{dis}}\right] \tag{16}$$

where σ is the self-discharging rate of the battery bank which is 0.0058% per hour for Lead-acid batteries η_{ch} is the efficiency charging which is 90%, and η_{dis} is the efficiency of the discharging which is 90%.

III. METHODOLOGY

This section presents the proposed model for optimal sizing of a Wind-PV grid-connected HRES.

A. Objective Function

This paper aims to design a system that always provides the base load at any time with the lowest possible cost. The objective is to provide the base load during a year using predefined units of PV panels, WTs, and batteries. Thus, the objective function should be defined to minimize the total cost, consisting of the investment cost of each component multiplied by the number of used units of each component as (17).

$$\min C^{Total}=C_{PV}.N_{PV}+C_{WT}.N_{WT}+C_{Bat}.N_{Bat} \tag{17}$$

Where, C^{Total} is the total investment needed, C_{PV} is the investment cost of each PV panel unit, N_{PV} is the number of PV panels needed, C_{WT} is the investment cost of a WT unit, N_{WT} is the number of needed WT units, C_{Bat} is the investment cost of a battery unit, and N_{Bat} is the number of batteries needed.

B. Constraints

The proposed model is subject to some practical constraints guaranteeing the desired operating conditions. Constraint (18) is associated with providing the base load ($P_{design}(t)$).

$$P_g(t)+P_{dis}(t)=\frac{P_{design}(t)}{\eta_{inv}}+P_{ch}(t), \qquad t=1,...,8760 \tag{18}$$

In which,

$$P_g(t)=N_{WT}.p_w(t)+N_{PV}.p_{PV}(t) \tag{19}$$

where, $p_w(t)$ and $p_{PV}(t)$ are the generation output of a PV and WT unit in each hour of the year, respectively. η_{inv} is the inverter's efficiency, which is considered 95%.

The other constraints concern the operating state of the battery bank. These constraints are associated with its state of charge, charging and discharging power, minimum state of charge, and maximum state of charge as follows:

$$SOC(t)=SOC(t-1)*(1-\sigma)+\left[\eta_{ch}P_{ch}(t)-\frac{P_{dis}(t)}{\eta_{dis}}\right] \tag{20}$$

$$SOC_{\min}\le SOC(t)\le SOC_{\max} \tag{21}$$

$$0\le P_{ch}(t)\le S_{ch}(t).P_{ch}^{\max} \tag{22}$$

$$0\le P_{dis}(t)\le S_{dis}(t).P_{dis}^{\max} \tag{23}$$

$$S_{ch}(t)+S_{dis}(t)\le 1 \tag{24}$$

Equations (22) to (24) control the charging and discharging power of BESS and stops BESS from charging and discharging simultaneously. $S_{dis}(t)$ and $S_{dis}(t)$ are binary variables that set the charging or discharging mode of the battery.

The other constraints are associated with the minimum and maximum number of each component as follows:

$$0\le N_{PV}\le N_{PV}^{\max} \tag{25}$$

$$0\le N_{WT}\le N_{WT}^{\max} \tag{26}$$

$$0\le N_{Bat}\le N_{Bat}^{\max} \tag{27}$$

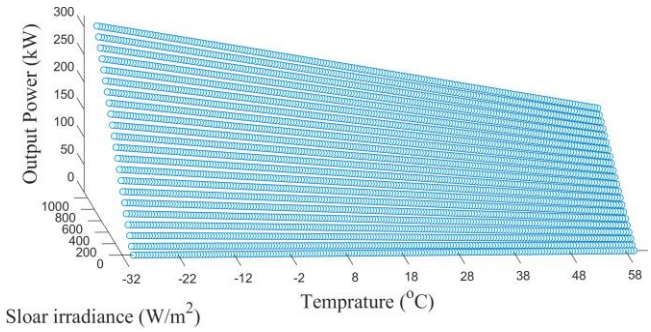

Figure 2: Maximum PV power for each solar radiation and temperature

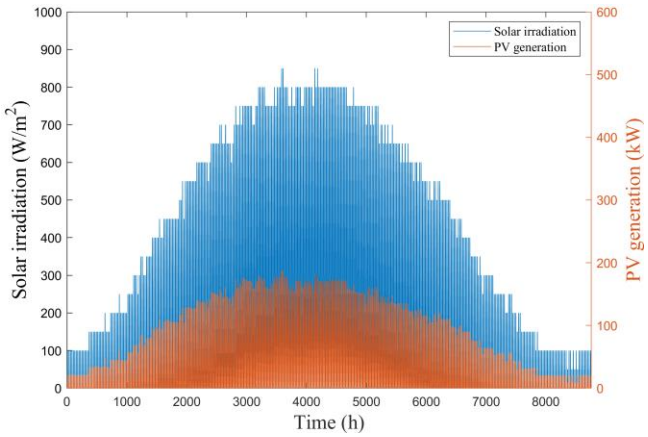

Figure 3: PV unit power output in Helsinki region

IV. Input Data

This section presents geographical data and components used in this paper for simulation. First, geographical data for ambient temperature, solar irradiation, and wind speed will be gathered. Then, a unit for each of the components (1MW for WT and 200kWp for PV) will be selected and their characteristics are presented.

A. Geographical Data

Ambient temperature, solar irradiation, and wind speed are the data needed for simulation. These data were obtained from [17] for the Helsinki region in 2019 and are used in the following to determine PV panel and wind turbine units.

B. PV Panel

The associated data for the selected PV unit is provided in Table A1. The other characteristics used for simulation can be found in [18]. Figure 2 presents the maximum power point of the used PV panel associated with solar irradiation and ambient temperature, which are calculated using Matlab/Simulink. These data will be used to calculate PV output using the given geographical data for the Helsinki region. The output power for the single PV panel and solar radiation in the Helsinki region is presented in Figure 3. Using these values, optimal sizing will be carried out.

C. Wind Turbine

The second RES used in this system is a WT. The output power table of the WT is shown in Table A2, and more data can be found in [19]. Based on Table A2 and wind speed in the Helsinki region, the output power of WT over a year is shown in Figure 4.

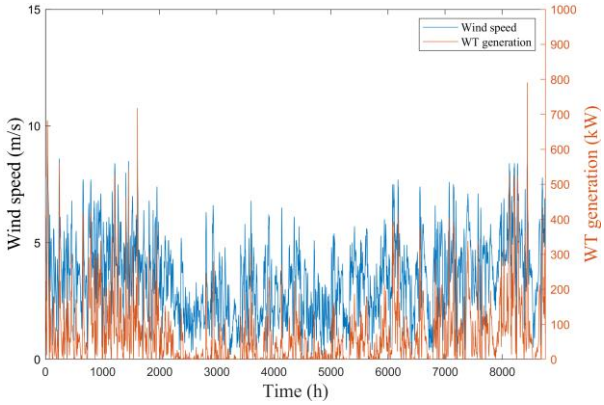

Figure 4: Wind turbine unit power output in Helsinki region

D. Battery Storage System

The last component used in this modeling is BESS. The used battery unit data is presented in Table A3.

V. Simulation Results

Using the developed model and the input data, the simulation has been carried out for optimal sizing of 3 main components of a Wind-PV grid-connected HRES under three scenarios for the base load conditions. In Scenario 1, the power injection level is limited to a constant level. In Scenario 2, the HRES can inject more power than the base level, while in Scenario 3, the injection level is limited to 10% higher and lower than the base load. The results for these scenarios with different levels of base load without any generation curtailment are presented in Table A4.

As the results show, Scenario 1 results in a significantly higher investment cost, for instance, in 1MW base load, Scenario 1 respectively requires 3.19 and 2.37 times the investment of Scenario 2 and Scenario 3. In this scenario, the portion of investment related to the BESS is higher than that of other scenarios. For instance, in 1MW base load, in Scenario 1, over 90% of the total investment is for BESS. However, in Scenario 2 and Scenario 3 this is 58.91% and 77.05% of the total investment, respectively. Also, Table A4 shows that investment cost per MW decreases when the capacity of the HRES is increased. For instance, investment cost per MW decreases from 144.91 M€/MW for 1 MW base load to 95.58 M€/MW for 8 MW base load in Scenario 1. On the other hand, in Scenario 2, the investment cost drops significantly compared to Scenario 1 and is less than that of Scenario 3. However, this results in a huge peak power injection to the grid. Also, the portion of investment related to the BESS is the least in this scenario. In Scenario 3, investment costs are considerably less than in Scenario 1 and slightly higher than those of Scenario 2.

Table A5 presents the results for HRES sizing with generation curtailment. For all scenarios, the investment cost and the portion of investment related to the BESS are dropped. The comparison between scenarios shows that the configuration of the system for Scenarios 1 and 2 are the same, i.e., the same size for PV, WT, and BESS is achieved, and only generation curtailment plays a role in satisfying the conditions. Due to the high investment cost of BESS, in the optimal solution for Scenario 2, the excess generation is curtailed to match Scenario 1 constraints. On the other hand, surprisingly,

the total investment cost in Scenario 3 is the least. In this scenario, due to the ability to decrease the load below average, the system has more flexibility to satisfy minimum SOC. Hence, smaller storage can be used in this scenario to reduce the investment costs.

To investigate the effectiveness of an HRES in comparison to a single RES system, Figure 5 shows the capital cost and percentage of the capital cost related to BESS for Scenario 3 without generation curtailment for three systems. As can be seen, the capital cost for HRES is significantly less than single RES systems and needs less BESS to provide the base load. For instance, to supply 10MW of the base load, the investment cost of HRES is 91.3% and 90.9% less than only PV and only WT RES system, respectively. The outcomes prove that combining WT with PV panels results in a more economical system, even for countries like Finland with long winters.

VI. CONCLUSION

In this paper, the feasibility of using HRES to supply base load for a power system was investigated. For this purpose, a model was developed to find the optimal size of three main components of an HRES, including PV panels, WTs, and BESS. Based on the environmental factors, the hourly production of a 200kwp PV panel and 1MW WT was calculated as a sizing unit.

The results indicated that adding flexibility to the power injection, not restricting the system from injecting the designed power to the grid at all times, reduced the investment costs by up to 60%. Furthermore, adding generation curtailment lowers the investment cost by adding more generation units and having less BESS. Moreover, an HRES needs less investment cost compared to the case when only a single RES system was considered. For instance, to supply a 10MW average base load, an HRES requires about 8.7% and 9.1% of the investment costs needed for only PV or only WT RES systems, respectively. Despite the significant superiority of an HRES over a single RES system to supply the base load, still, a large-scale EESS is required to supply the base load using RESs.

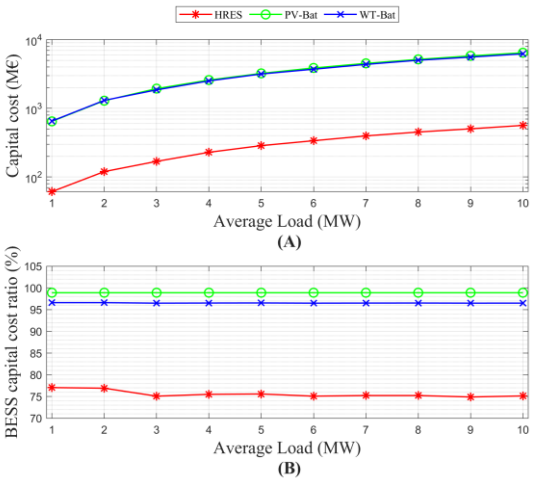

Figure 5: (A) Capital cost for average loads (Logarithmic scale), (B) Percentage of capital the cost related to BESS

REFERENCES

[1] E.--E. Commission and others, "Regulation (EU) 2021/1119 of the European Parliament and of the Council of 30 June 2021 establishing the framework for achieving climate neutrality and amending Regulations (EC) No 401/2009 and (EU) 2018/1999 ('European Climate Law'), document 32021R1119," *Off. J. Eur. Union*, vol. 243, pp. 1–17, 2021.

[2] M. Engin, "Sizing and Simulation of PV-Wind Hybrid Power System," *Int. J. Photoenergy*, vol. 2013, pp. 1–10, 2013, doi: 10.1155/2013/217526.

[3] K. Anoune, A. Laknizi, M. Bouya, A. Astito, and A. Ben Abdellah, "Sizing a PV-Wind based hybrid system using deterministic approach," *Energy Convers. Manag.*, vol. 169, pp. 137–148, Aug. 2018, doi: 10.1016/j.enconman.2018.05.034.

[4] K. Sopian, M. Z. Ibrahim, W. R. Wan Daud, M. Y. Othman, B. Yatim, and N. Amin, "Performance of a PV–wind hybrid system for hydrogen production," *Renew. Energy*, vol. 34, no. 8, pp. 1973–1978, Aug. 2009, doi: 10.1016/j.renene.2008.12.010.

[5] L. Arribas, L. Cano, I. Cruz, M. Mata, and E. Llobet, "PV–wind hybrid system performance: A new approach and a case study," *Renew. Energy*, vol. 35, no. 1, pp. 128–137, Jan. 2010, doi: 10.1016/j.renene.2009.07.002.

[6] H. Belmili, M. Haddadi, S. Bacha, M. F. Almi, and B. Bendib, "Sizing stand-alone photovoltaic–wind hybrid system: Techno-economic analysis and optimization," *Renew. Sustain. Energy Rev.*, vol. 30, pp. 821–832, Feb. 2014, doi: 10.1016/j.rser.2013.11.011.

[7] Y. Sawle, S. C. Gupta, and A. Kumar Bohre, "PV-wind hybrid system: A review with case study," *Cogent Eng.*, vol. 3, no. 1, p. 1189305, Dec. 2016, doi: 10.1080/23311916.2016.1189305.

[8] L. Al-Ghussain and O. Taylan, "Sizing methodology of a PV/wind hybrid system: Case study in cyprus," *Environ. Prog. Sustain. Energy*, vol. 38, no. 3, p. e13052, May 2019, doi: 10.1002/ep.13052.

[9] T. Sarkar, A. Bhattacharjee, H. Samanta, K. Bhattacharya, and H. Saha, "Optimal design and implementation of solar PV-wind-biogas-VRFB storage integrated smart hybrid microgrid for ensuring zero loss of power supply probability," *Energy Convers. Manag.*, vol. 191, pp. 102–118, Jul. 2019, doi: 10.1016/j.enconman.2019.04.025.

[10] F. Al-Turjman, Z. Qadir, M. Abujubbeh, and C. Batunlu, "Feasibility analysis of solar photovoltaic-wind hybrid energy system for household applications," *Comput. Electr. Eng.*, vol. 86, p. 106743, Sep. 2020, doi: 10.1016/j.compeleceng.2020.106743.

[11] Y. Zhang, J. Lian, C. Ma, Y. Yang, X. Pang, and L. Wang, "Optimal sizing of the grid-connected hybrid system integrating hydropower, photovoltaic, and wind considering cascade reservoir connection and photovoltaic-wind complementarity," *J. Clean. Prod.*, vol. 274, p. 123100, Nov. 2020, doi: 10.1016/j.jclepro.2020.123100.

[12] K. Anoune *et al.*, "Optimization and techno-economic analysis of photovoltaic-wind-battery based hybrid system," *J. Energy Storage*, vol. 32, p. 101878, Dec. 2020, doi: 10.1016/j.est.2020.101878.

[13] A. Naderipour *et al.*, "Comparative evaluation of hybrid photovoltaic, wind, tidal and fuel cell clean system design for different regions with remote application considering cost," *J. Clean. Prod.*, vol. 283, p. 124207, Feb. 2021, doi: 10.1016/j.jclepro.2020.124207.

[14] G. Notton, V. Lazarov, and L. Stoyanov, "Optimal sizing of a grid-connected PV system for various PV module technologies and inclinations, inverter efficiency characteristics and locations," *Renew. Energy*, vol. 35, no. 2, pp. 541–554, Feb. 2010, doi: 10.1016/j.renene.2009.07.013.

[15] W. Zhou, H. Yang, and Z. Fang, "A novel model for photovoltaic array performance prediction," *Appl. Energy*, vol. 84, no. 12, pp. 1187–1198, Dec. 2007, doi: 10.1016/j.apenergy.2007.04.006.

[16] R. Belfkira, L. Zhang, and G. Barakat, "Optimal sizing study of hybrid wind/PV/diesel power generation unit," *Sol. Energy*, vol. 85, no. 1, pp. 100–110, Jan. 2011, doi: 10.1016/j.solener.2010.10.018.

[17] N. S. R. Databse, "No Title," 2023. https://nsrdb.nrel.gov/data-viewer/

[18] N. Anani and H. Ibrahim, "Adjusting the Single-Diode Model Parameters of a Photovoltaic Module with Irradiance and Temperature," *Energies*, vol. 13, no. 12, p. 3226, Jun. 2020, doi: 10.3390/en13123226.

[19] WinWind, "WWD-1 1 MW wind turbine Technical specification." https://d3icht40s6fxmd.cloudfront.net/sites/default/files/attachments/technical_specification_wwd1.pdf

VII. APPENDIX

This appendix provides the tables and data used and presented in this paper.

Table A1 to Table A3 gives the data associated with PV panel specification, wind turbines' generation characteristics, and battery storage system characteristics, respectively. Furthermore, Table A4 presents the obtained data related to the total investment cost, the size of each HRES component, the portion of total investment related to the battery energy storage system, and the supplied power to the grid by the system when there is no generation curtailment. On the other hand, Table A5 presents the above-mentioned results for the HRES system when there is the possibility of generation curtailment.

TABLE A1. PV PANEL SPECIFICATION

P_r (W)	$\alpha_{P_{mpp}}$ (%)	$\alpha_{V_{mpp}}$ $(mV/°C)$	$\alpha_{I_{SC}}$ $(mA/°C)$	$\alpha_{V_{OC}}$ $(mV/°C)$	$NCOT$ $(°C)$
200	-0,52	-167	1,4	-161	46

TABLE A2. WIND TURBINE GENERATION CHARACTERISTIC

Wind Speed (m/s)	Output Power (kW)	Wind Speed (m/s)	Output Power (kW)
3	22	15	1019
4	66	16	1019
5	129	17	1019
6	213	18	1019
7	325	19	1019
8	461	20	1019
9	628	21	1019
10	809	22	1019
11	991	23	1019
12	1019	24	1019
13	1019	25	1019
14	1019	26	0

TABLE A3. BATTERY UNIT CHARACTERISTIC

Nominal Capacity (Ah)	Voltage (V)	DOD (%)	Efficiency (%)	Capital Cost (€)
104	12	80	85	206,4

TABLE A4. HRES COMPONENT'S SIZE WITHOUT GENERATION CURTAILMENT

Output Power Condition (MW)	Total Cost (M€)	P PV (MW)	P WT (MW)	P Bat (MWh)	BESS Cost Ratio (%)	P Min (MW)	P Mean (MW)	P Max (MW)
1 (Scenario 1.1)	144.94	3	9	789.33	90.06	1	1	1
4 (Scenario 1.2)	384.38	11.6	36	1978.08	85.11	4	4	4
8 (Scenario 1.3)	764.67	22.8	73	3925.719	84.91	8	8	8
> 1 (Scenario 2.1)	45.42	3.4	12	161.78	58.91	1	1.31	61.98
> 4 (Scenario 2.2)	181.47	13.2	46	663.82	60.50	4	5.03	99.95
> 8 (Scenario 2.3)	362.62	26	91	1335.80	60.92	8	9.90	107.60
0.9 < P < 1.1 (Scenario 3.3)	61.19	2.6	9	285.08	77.05	0.9	0.96	1.1
3.6 < P < 4.4 (Scenario 3.3)	229.04	11.8	35	1045.56	75.50	3.6	4.00	4.4
7.2 < P < 8.8 (Scenario 3.3)	452.00	24.8	69	2055.71	75.22	7.2	8.12	8.8

TABLE A5. HRES COMPONENT'S SIZE WITH GENERATION CURTAILMENT

Output Power Condition (MW)	Total Cost (M€)	P PV (MW)	P WT (MW)	P Bat (MWh)	BESS Cost Ratio (%)	P Min (MW)	P Mean (MW)	P Max (MW)
1 (Scenario 1.1)	45.42	3.4	12	161.78	58.91	1	1	1
4 (Scenario 1.2)	181.38	13.2	46	663.30	60.48	4	4	4
8 (Scenario 1.3)	362.62	26	91	1335.80	60.92	8	8	8
> 1 (Scenario 2.1)	45.42	3.4	12	161.78	58.91	1	1.31	62.06
> 4 (Scenario 2.2)	181.38	13.2	46	663.30	60.48	4	5.03	99.96
> 8 (Scenario 2.3)	362.62	26	91	1335.80	60.92	8	9.90	113.41
0.9 < P < 1.1 (Scenario 3.3)	40.86	3	11	144.25	58.4	0.9	1.02	1.1
3.6 < P < 4.4 (Scenario 3.3)	163.29	12	41	599.74	60.74	3.6	4.09	4.4
7.2 < P < 8.8 (Scenario 3.3)	326.36	23.4	82	1201.45	60.88	7.2	8.17	8.8